International Journal of GEOMATE, Jan., 2024 Vol.26, Issue 113, pp.74-81
ISSN: 2186-2982 (P), 2186-2990 (O), Japan, DOI: https://doi.org/10.21660/2024.113.g13226
Geotechnique, Construction Materials and Environment

THREE-DIMENSIONAL PHYSICAL MODELING ON SOFT SOIL IMPROVEMENT BY RIGID INCLUSIONS

Parita Bunchob[1], Chainarong Songsiri[1], Palinee Sumitsawan[2], Kwansirinapa Thanawong[2] and *Suriyavut Pra-ai[2]

[1]Civil Engineering Department, School of Engineering, University of Phayao, Thailand
[2]RS2GH Research Unit, School of Engineering, University of Phayao, Thailand

*Corresponding Author, Received: 15 June 2023, Revised: 15 Dec. 2023, Accepted: 18 Dec. 2023

ABSTRACT: The technique of vertical rigid inclusions has been widely used to improve the soft soil problem due to its low cost and resulting small differential and total settlements. Obviously, experimental studies on rigid inclusion improvement systems have been conducted by several researchers. This paper presents an experimental study focusing on the mechanisms taking place in a granular platform supported by piles in soft soil under monotonic loading. An original three-dimensional laboratory model was developed. The model contained 16 rigid piles, and the compressible soil was explicitly simulated by a soft material (a mixture of polypropylene balls with granular soil). Settlement accumulation and an increase in the load transmitted to the piles or pile caps were observed during the loading application. Based on the experimental results, an increase in pile diameter played an important role in load transfer mechanisms, including the total settlement. The importance of this campaign in terms of parametric study will constitute rich experimental data in the context of soft soil improvement reinforced by rigid inclusions to develop and validate the numerical part.

Keywords: Small-scale model, Rigid inclusions, Load transfer platform, Geosynthetics

1. INTRODUCTION

Soft soils always pose significant challenges for various engineering applications, such as the construction of foundations, embankments, and transportation infrastructure. Normally, soft soils are characterized by low shear strength, high compressibility, and excessive settlements, which can lead to structural failures. To overcome these challenges and enhance the load-bearing capacity of soft soil, various ground improvement techniques have been developed and implemented. One such technique that has gained considerable attention in recent years is the use of rigid inclusions or piled embankments ([1-10]). The concept of using rigid inclusions for soft soil improvement has been extensively studied. Rigid inclusions are vertical elements typically made of materials, such as stone columns and concrete piles, which are replaced into the soft soil to increase its stiffness and strength. These inclusions, which can have caps or enlarged heads, act as load-bearing elements, transferring the applied load to more competent layers of the soil stratum.

An embankment or a load transfer platform (LTP) is normally constructed over the soft soil layer reinforced by rigid inclusions, where shearing mechanisms termed the arching effect mobilize. The arching effect, which partially transmits the load from the surface to piles, allows for the reduction and homogenization of the surface settlements. To enhance load transfer mechanisms and minimize settlements, geosynthetics are effectively incorporated into earth platforms combined with the rigid inclusion–reinforced soft soil as an integrated system ([3-4], [6]). It is found that the influence of geosynthetic reinforcement on the load transfer mechanism becomes more complex when multi-layers of geosynthetic reinforcement are installed within the LTP layer ([6], [11]).

Numerous laboratory and field studies have been conducted to investigate the behavior of soft soil improved by rigid inclusions and geosynthetic layers ([7], [9-11]). For instance, various experimental and numerical investigations of soft soil reinforced by vertical rigid inclusion have been presented under the framework of the ASIRI French National Research Program [10].

Physical models can serve as a tool to validate and calibrate numerical models employed to simulate the behavior of soft soil reinforced by rigid inclusions. Several studies have focused on evaluating the load transfer mechanisms of the inclusions. The load-settlement responses have also been described [9-13]. However, these models cannot respect the real-scale structure. To overcome the scaling effect, centrifuge tests on piled embankments, which can be representative of the behavior of a full-scale structure, named prototype, were performed by many researchers such as Blanc et al. [5], Okyay et al. [16], and Fagundes et al. [17]. The behavior of compressible soils reinforced by vertical rigid inclusions is also studied by experiments on reduced-scale 3D centrifuged models. These tests make it possible to apply stress levels of the same order as in real cases. However, they present other limitations, such as the difficulty of representing all the materials explicitly ([16]).

Analytical methods, in which the soil arching and tension membrane approaches are described, have been presented to analyze the load-deformation behavior of geosynthetic reinforcement in a pile-supported embankment ([3-4], [19]). Numerical modeling techniques have played an important role in advancing the understanding of rigid inclusion-reinforced soft soil behavior. These studies can provide insights into the complex interactions between the inclusions and the surrounding soil, allowing for the prediction of various performance parameters ([18-20]). It has been conceived that many such mechanisms, e.g., the use of granular layer and geosynthetic reinforcement, are sophisticated and their description by means of analytical design scheme remains problematic.

This paper will describe a series of experimental observations on soft soil reinforcement by rigid inclusions subjected to monotonic loading using a 3D small-scale physical model. The originality of this model lies in its modularity in terms of geometry, materials, and boundary conditions. The effects of cover ratio and geosynthetic layer laid over the soft soil, preloading and boundary conditions will preliminarily be described.

2. RESEARCH SIGNIFICANCE

Small-scale physical models can provide an opportunity for performing parametric studies and optimization experiments. By alternating certain parameters (e.g., spacing and length of inclusions, or soil properties), researchers can assess their influence on the behavior of the reinforced soil system. The objective of this model is not to quantitatively simulate the behavior of a real structure (i.e., the rules of similarity are not all strictly respected) but aims to better understand the mechanisms which develop within the massif and more precisely in the LTP layer, to analyze the effect of geosynthetic reinforcement and to better understand the interaction mechanisms between these various parts of the structure. These model tests will contribute significantly to enhancing the understanding of the load transfer mechanisms and facilitate the constitution of an experimental campaign of cyclic loading studies and evaluation of analytical and computational approaches.

3. EXPERIMENTAL PROCEDURE

2.1 1-g Small Scale

A small-scale physical model which has many advantages (e.g., highlighting mechanisms, obtaining experimental results to calibrate numerical models, and possibly performing tests until failure), can provide a valuable means to obtain insights and understanding of soft soil reinforced by rigid inclusions. One of the major drawbacks is to satisfy the rules of similarity, in order to apply the results observed on the small model to the full-scale problem. These rules are established from the general equations of mechanics, the conservation of mass equation and the laws of material behaviors. Although this small-scale model did not respect the real scale structure, the experiments will aid in optimizing the design of inclusion systems, and determining the most effective parameters for achieving the load transfer mechanism and settlement control.

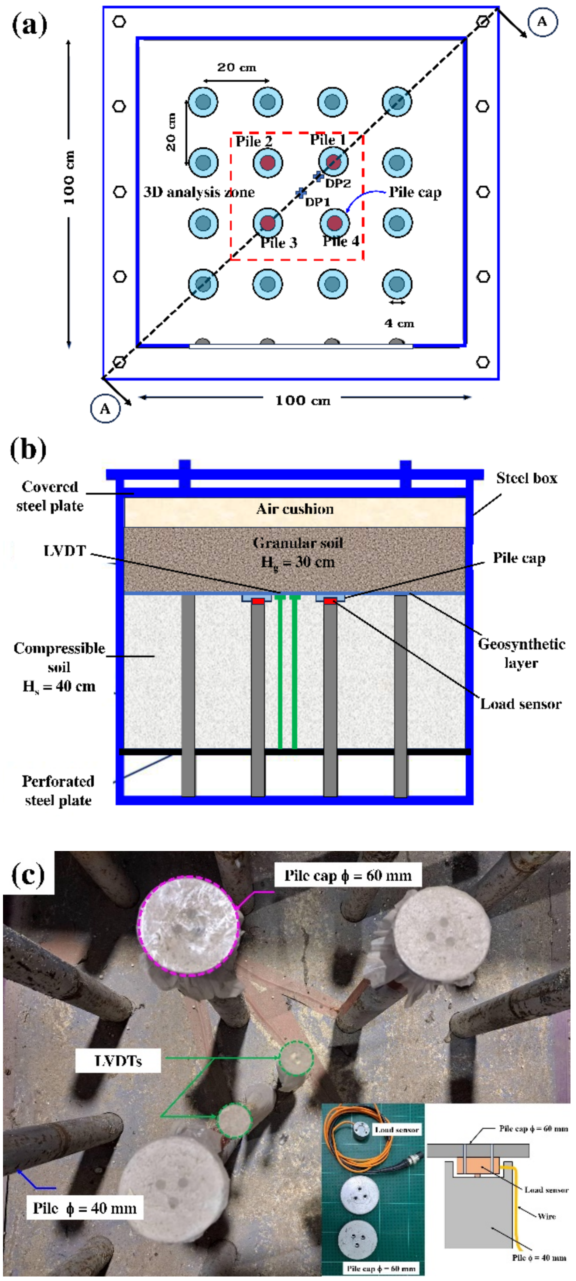

Fig.1 (a) schematic plane view of test set-up; (b) test set-up with instrumentation; (c) force sensor positioning system at the pile head.

Fig.1a and 1b show the small-scale physical model in this study. Based on the experimental observations performed by Houda et al. [12-14] and Insoog et al. [15], this model is under the normal gravity at 1/10th scale on the lengths. The model is made of a steel tank of 1x1 m^2, containing 16 steel pipes with a diameter of 40 mm and a height of 600 mm. The steel pipes were filled with a concrete mixture in order to be sufficiently rigid. This can be assumed that there is no insignificant deformation on steel pipes. The piles were set in a square mesh of 200 mm, center to center.

For the purposes of 3-D model test, the load transfer mechanism on each pile (F1, F2, F3 and F4) can be measured by installing the load sensors at the top of the four-central piles. Ensuring stability, the installation involved cutting the pile head to secure and immobilize the sensors. In case of an enlarged recovery ratio, the force sensor at the pile head with a diameter of ϕ = 60 and 80 mm is surmounted by a transmission cap, which is an aluminum part in order to transmit the entire applied load to the measuring pin of the sensor (Fig.1c). As these four piles were situated among the others, the effect of boundaries could be neglected. In the case of enlarged pile caps, steel caps with defined diameters were positioned atop the load sensors. Fig.2 shows the recovery ratio (α) which expresses the cross-section area of the pile or pile cap (A_p) over the area of the elementary grid (A). This recovery ratio can be written as

$$\alpha = \frac{A_p}{A} \tag{1}$$

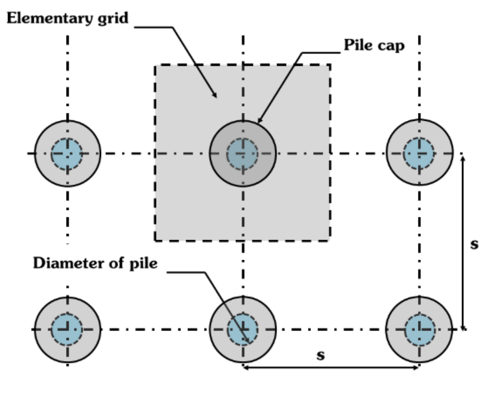

Fig.2 Definition of recovery ratio (α)

To capture displacements, two displacement sensors (DP1 and DP2) were placed along the diagonal line connecting the piles. The displacement sensors are connected to rods passing through the compressible soil to its surface. Steel discs were attached to these rods, on the surface of the compressible soil mass, in order to imprint the settlement experienced at these points. To prevent any obstacle from the friction of the compressible soil, the rods were enclosed in plastic sheaths as they passed through the compressible soil. Thus, the displacements measured by the displacement sensors correspond to the surface settlement of the compressible soil mass.

2.2 Tested Materials

For investigating the load transfer mechanism in the laboratory, several materials were used to represent real soft soil (e.g., foam cushion [3-4], polyurethane foam (PU) [7], a mixture of fine sand, polystyrene balls, and water, [12-15]). To facilitate the sample preparation, the compressible soil used in this study was made of a mixture of polystyrene balls, sand, and water ([15]). A mixture of sand: water: polystyrene balls at 40: 4: 1 by weight was prepared and installed in the steel tank with the density of 4.5 kN/m^3. From the oedometer test, this sample can represent compressibility characteristics (i.e., compressibility index, C_c) similar to real soft soil. The LTP layer laid on the soft soil was composed of dry sand which was derived from Chiang Rai province in the north of Thailand. This sand was prepared with an average unit weight of 16.7 kN/m^3 providing a friction angle of 43°. Fig. 3 illustrates an example of tested materials used in this study and their grain size. A woven geotextile (Model TS20, see Fig.4) of which the properties were shown in Table 1 was employed to investigate the effect of the load transfer mechanism.

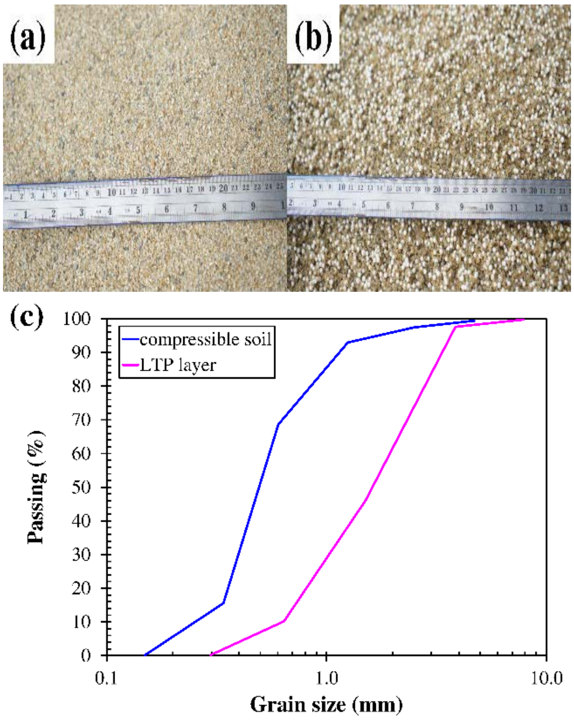

Fig.3 (a) LTP layer; (b) compressible soil made of a mixture of polystyrene balls, sand, and water; (c) grain size distribution of compressible soil and LTP layer.

Fig.4 Woven geotextile (Model TS20) used in this study.

Table 1 Mechanical properties of Polyfelt TS20 Woven Geotextiles used in this study.

Property	Unit	Value
Tensile strength (avg.) ISO 10319	kN/m	20
Tensile elongation (MD/CD) ISO 10319	%	75/35
Performance energy calculated	kN/m	25
CBR puncture strength ISO 12236	N	1500

2.3 Experimental Setup

In each testing session, adherence to a meticulous experimental protocol is imperative, outlining the specific steps for assembling and situating sensors and materials in the model. Fig. 5 provides a visual representation of the various stages involved in preparing for a test. The compressible soil was prepared with the tamping method. Once the desired thickness and density were established, a required weight of a mixture of sand, water and polystyrene balls was introduced into the steel tank and compacted. The dumping process aimed for a uniform density, with careful leveling at the upper level of the piles. To prevent contamination of the compressible soil by the LTP layer, a thin plastic sheet was positioned on the surface, strategically perforated at the pile heads to prevent the development of a membrane effect during differential settlement between the compressible soil and the piles. In the case of geosynthetic reinforcement, a layer of geotextile was overlaid the compressible soil.

The LTP layer was constructed in successive layers of 10 cm thickness, with the pluviation method and slight compaction of each layer following the same procedure for each test. Upon completion of sample preparation and instrument installation, the model was sealed with a protective steel plate to protect against the deformation induced by surface loading (Fig.6). The application of surface loading can be performed via an air cushion laid on the LTP layer under the controlled pressure system. This procedure can distribute a uniform load to the system.

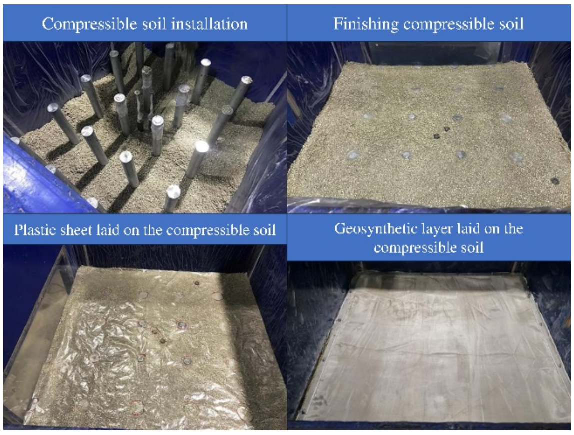

Fig.5 Procedure of sample preparation

Fig.6 Final stage of the model setup prior to surface loading application

Table 2 Tested program

Test	Recovery ratio, α (%)	Reinforcement
MS-4	3.14	-
MS-6	7.07	-
MS-8	12.56	-
MS-4R	3.14	Polyfelt TS20
MS-6R	7.07	Polyfelt TS20
MS-8R	12.56	Polyfelt TS20

4. RESULTS AND DISCUSSION

In this paper, different test configurations were performed. The test with geosynthetic reinforcement and the others without geosynthetic reinforcement will be investigated. Table 2 summarizes the test program in which a reference test was performed without a geosynthetic layer and enlarged pile head

(MS_4 with α = 3.14%). After installing the LTP layer, a consolidation period of twelve hours was maintained. Then, the surface loading (P_m) will be applied. In this study, three levels of P_m (i.e., 5, 15 and 25 kPa) will be performed. In each level loading, three hours of consolidation was kept. The forces transmitted to the piles are measured by force sensors integrated with the heads of the four piles at the center of the group.

Fig. 7 illustrates the forces Fi (i ranging from 1 to 4) measured on the pile head over time. With an incremental application of surface loading, there was a proportional increase in the forces acting on the head of all four piles. The value of Fi for each pile exhibited a maximum difference of 8 % compared to the average force across all piles, suggesting a relatively uniform distribution of surface loading.

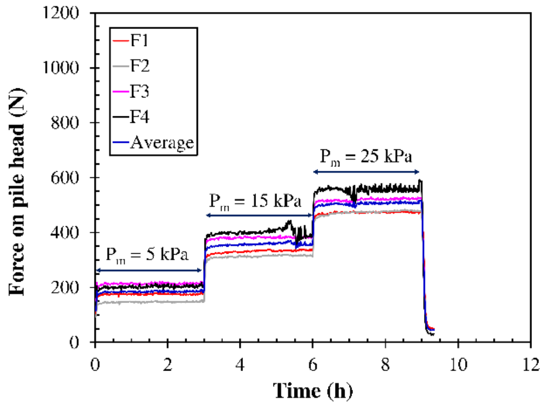

Fig.7 Force measured on each pile head during the application of surface loading for the test MS-4.

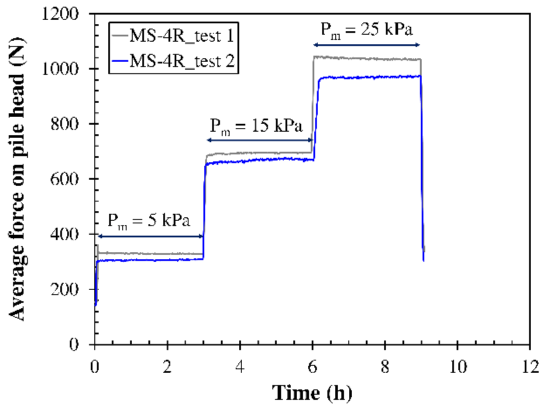

Fig.8 Average force measured on pile head during the application of surface loading for the test MS-4R.

To validate the device's reproducibility and the accuracy of the force sensors, Fig.8 depicts the average force on the pile head for two MS_4R tests. A noticeable but minor difference in the measured force on the pile head was observed when subjected to a surface loading of 25 kPa. Despite this disparity, it was within an acceptable range, confirming the consistency and reliability of both the device and the force sensors.

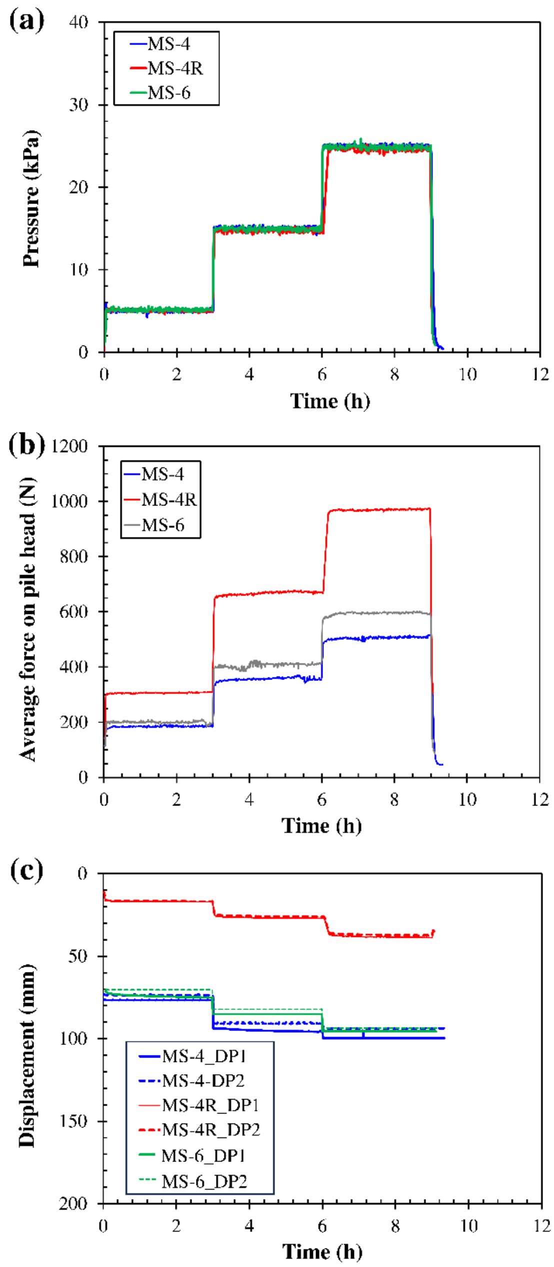

Fig.9 Monotonic test results for the test MS-4, MS-4R and MS-6

Fig.9 typically illustrates the response of the tests MS-4, MS-4R and MS-6 under monotonic loading. The application of surface loading in each test confirmed the consistency of the control system. Increasing the recovery ratio (α) significantly enhanced load transfer to the pile head and resulted in reduced overall settlements. In the absence of a geosynthetic layer, during the initial step at P_m = 5 kPa, the average forces on piles exhibited a slight increase as α increased from 3.14% to 7.07%. However, as P_m increased to 15 and 25 kPa, a notable disparity in the average force on the pile head was observed for the test with an enlarged pile cap (Fig.9b). Conversely, in the case of geosynthetic reinforcement, the average force on the pile head was more pronounced. Comparing MS-4 and MS-4R, the average force measured on the pile head for MS-4R was approximately twice as high as that for MS-4 at the second and third step of loading, P_m = 15 and 25 kPa.

The settlement at the compressible soil/LTP interface was quantified using two displacement sensors (DP1 and DP2) placed along the diagonal of the central 3D analysis zone. The sensor placed in the center of the analysis zone between the piles was DP1 while DP2 was located next to the pile. The presence of the geosynthetic layer facilitated a more uniform load distribution across the pile head, resulting in a significant reduction in settlement. Interestingly, the geosynthetic layer appeared to be more effective than the pile head in reducing settlements (Fig.9c). At the end of the consolidation period, the settlements measured for MS-4 and MS-8 were DP1 = 76.22 and 67.20 mm, respectively. By enhancing load transfer, both the pile cap and geosynthetic layer contributed to the overall settlement reduction in the piled embankment. MS-4R, featuring a geosynthetic layer, exhibited a significantly diminished settlement of DP1 = 11.41 mm after a 12-hour consolidation period. This substantial settlement reduction in the test with the geosynthetic layer was also observed during the sand layer installation stage.

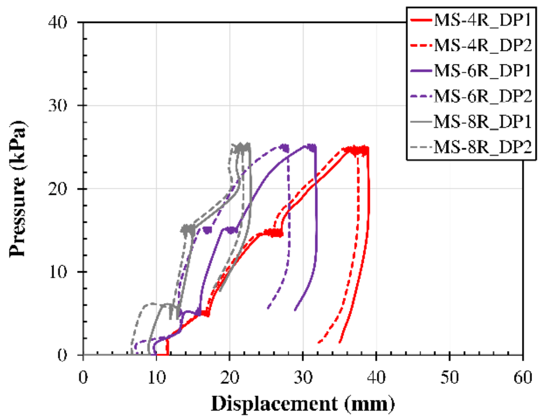

Fig.10 Evolution of settlements DP1 and DP2 with the pressure applied to the surface for the tests with geosynthetic layer.

Fig. 10 presents the evolution of settlements during different monotonic loading stages for tests incorporating the geosynthetic layer. Despite variations in recovery ratios among the tests, the initial settlement attributable to the installation of the LTP layer remained relatively consistent, ranging from 7-12 mm. This uniform settlement trend could be linked to the influence of the geosynthetic layer. As surface loading increased, tests with lower recovery rations, such as MS-4R with α = 3.14%, exhibited more pronounced total settlements.

To evaluate load transfer on the pile, the efficiency of the system can be expressed as the ratio between the load measured on the pile or pile cap (F) and the total load above the piles within the elementary grid depicted in Fig.2 (i.e., the weight of LTP layer, W + surface loading, P):

$$E = \frac{F}{W + P} \tag{2}$$

After the stage of construction of the LTP layer, the efficiency as a function of α at this stage can be shown in Fig.11. A slight increase in efficiency for the test with the geosynthetic layer was observed when performing the tests with a low value of α. In the case of α = 12.56, the difference in efficiency of 11 % could be observed between the tests with and without the geosynthetic layer.

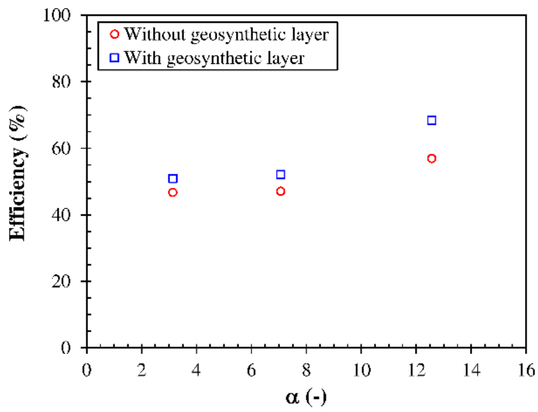

Fig.11 Influence of recovery ratio (α) on efficiency before applying the surface loading.

Fig.12 summarizes the average system efficiency across all tests, revealing the important roles played by the recovery ratio and the presence of a geosynthetic layer in load transfer mechanisms. Notably, at the beginning of surface loading for each step, the forces measured on the pile heads did not increase coincidently. The rate of force increment on the pile heads lagged behind that of the surface loading, resulting in a reduction in the efficiency of the system.

Examining the effect of geosynthetic layer, the efficiency for the test performed with α = 3.14 % increased from 42.24 % to 77.26 % at P_m = 25 kPa. In the case of α = 12.56 %, an efficiency of 60.42 % was observed at P_m = 25 kPa. Notably, the reinforcement layer demonstrated greater effectiveness than an increase in the size of the pile cap. Test MS-8R exhibited a more pronounced efficiency, particularly during the initial step of loading at P_m = 5 kPa. However, when an increase in P_m to 25 kPa was applied, the efficiency of the system appeared to decrease. Nevertheless, in the case of the geosynthetic layer, an increase in α (MS-6 and MS-8) had no influence on the efficiency of the system at a higher level of P_m.

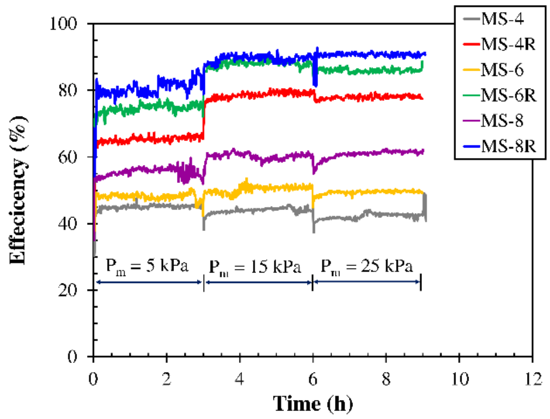

Fig.12 Evolution of the average efficiency at the pile head or pile cap of four central piles

5. CONCLUSION

In this study, although this small-scale model did not precisely replicate the real - scale structure, the primary focus was on validating reference tests. Based on the experimental results, an increase in pile diameter played a crucial role in load transfer mechanisms including the total settlement. The significance of this study lies in its potential for extensive parametric analysis, as it provides a wealth of experimental data pertaining to the improvement of soft soil through rigid inclusions. This dataset can be instrumental in shaping future experimental campaigns, particularly those involving cyclic loading tests, and validating numerical models.

In the context of monotonic test results serving as a reference, a layer of dry sand with a unit weight of 16.7 kN/m^3 and a friction angle of 43° was employed as the LTP layer. Following a 12-hour consolidation period, the application of surface loading induced the accumulation of settlement.

Tests incorporating an enlarged pile cap and a geosynthetic layer demonstrated the capacity to distribute loads more uniformly across the pile head, resulting in a significant reduction in settlement. This effect was particularly prominent when a low level of surface loading was applied. Interestingly, an increase in the recovery ratio exhibited no discernible impact on the system's efficiency at high levels of surface loading (P_m).

6. ACKNOWLEDGMENTS

This research project was supported by the Thailand science research and innovation fund and the University of Phayao under the contract No. FF66-RIM037. The authors are also grateful to Professor Daniel Dias and Professor Orianne Jenck at 3SR Laboratory, University of Grenoble for their valuable comments and suggestions.

7. REFERENCES

[1] Briançon L. and Simon B., 2011. Performance of pile-supported embankment over soft soil: full-scale experiment. J. Geotech. Geoenviron. Eng. Vol. 138, Issue 4, 2011, pp.551–561.

[2] Nuñez M., Dias D., Kastner R., and Poilpré C., Soft Ground Improved by Rigid Vertical Piles. Experimental and Numerical Study of Two Real Cases in France, International Conference on Case Histories in Geotechnical Engineering, 2008, 40.

[3] Van Eekelen SJM., Bezuijen A. and Van Tol A.F., Model experiments on piled embankments. Part I. Geotextiles and Geomembranes, Vol. 32, 2012, pp.69–81.

[4] Van Eekelen SJM., Bezuijen A. and Van Tol A.F., Model experiments on piled embankments. Part II. Geotextiles and Geomembranes, Vol. 32, pp.82–94.

[5] Blanc M, Rault G, Thorel L. and Almeida M., Centrifuge investigation of load transfer mechanisms in a granular mattress above a rigid inclusions network. Geotext Geometry, Vol. 36, 2013, pp.92–105.

[6] Van Eekelen SJM., Bezuijen A., Is 1+1=2? Results of 3D model experiments on piled embankments. In Proc. 10th International Conference on Geosynthetics (IGS-2014), 2014

[7] Kongkitkul W., Chaiyaporn U., Youwai S. and Jongpradist P., Role of geogrids in load transfer of pile-supported embankments. Ground Improvement, Vol. 165, Issue 14, 2012, pp.239-248.

[8] Briançon L, Dias D. and Simon S., (2015) Monitoring and numerical investigation of a rigid inclusions – reinforced industrial building. Canadian Geotechnical Journal, Vol. 52, 2015, pp.1–13.

[9] Van Eekelen SJM. and Han J., Geosynthetic-reinforced pile-supported embankment: state of the art. Geosynthetics International, Vol.27, Issue 2, 2020, pp.112-141

[10] IREX, Recommendations for the Design, Construction and Control of Rigid Inclusion Ground Improvements: ASIRI National Project.

Presses des Ponts, Paris, France, 2012.

[11] Girout R., Blanc M., Dias D. and Thorel L., Geosynthetic reinforcement of pile-supported embankment. Geosynthetics International, Vol. 25, Issue 1, 2018, pp. 1-13.

[12] Houda M., Jenck O. and Emeriault F., Physical evidence of the effect of vertical cyclic loading on soil improvement by rigid piles: a small-scale laboratory experiment using digital image correlation. Acta Geotechnica, Vol. 11, Issue 2, 2016, pp.325-356.

[13] Houda M., Jenck O. and Emeriault F., Rigid pile improvement under vertical cyclic loading: 1g laboratory small-scale modelling. Int. J. of Physical Modelling in Geotechnics, Vol.19, Issue 2, 2019, pp.89-103.

[14] Houda M., Jenck O. and Emeriault F., Soft soil improvement by rigid inclusions under verical cyclic loading: numerical back analysis. European Journal of Environmental and Civil Engineering, Vol. 25. Issue 3, 2018, pp.409-428.

[15] Insoog N., Pra-ai S., Pengjan C., Sumitsawan P. and Jenck O., Investigation of physical model on soft soil reinforced by rigid inclusions under cyclic loading. International Journal of GEOMATE, Vol.19, Issue 74, 2020, pp.37-43

[16] Okyay US., Dias D., Thorel L. and Rault G., Centrifuge modeling of a pile-supported granular earth-platform. Journal of Geotechnical and Environmental engineering, Vol.140, Issue 2, 2014, 04013015. doi: 10.1061/(asce)gt.1943-5606.0001004

[17] Fagundes D.F., Almeida MSS, Thorel L. and Blanc M., Load transfer mechanism and deformation of reinforced piled embankments. Geotextile and Geomembranes, Vol.45, pp. 2017, 1-10

[18] Pham, HV, and Dias D., 3D numerical modeling of rigid inclusion-improved soft soils under monotonic and cyclic loading-Case of a small-scale laboratory experiment. Appl. Sci. Vol.11, 2021, pp.1426.

[19] Pham TA., Load-deformation of piled embankments considering geosynthetic membrane effect and interface friction. Geosynthetics International, Vol. 27, Issue 3, 2020, pp 275-300

[20] Zhang J., Dias D., and Jenck O., 3D numerical modeling of a rigid inclusion reinforced railway embankment under cyclic loading. Transportation geotechnics, Vol.41, 2023, pp.101003